Spatiotemporal Patterns of Cortical Fiber Density in Developing Infants, and Their Relationship With Cortical Thickness

Gang Li,[1] Tianming Liu,[2] Dong Ni,[3]* Weili Lin,[1] John H. Gilmore,[4] and Dinggang Shen[1,5]*

[1]*Department of Radiology and BRIC, University of North Carolina at Chapel Hill, North Carolina*
[2]*Department of Computer Science and Bioimaging Research Center, The University of Georgia, Athens, Georgia*
[3]*Department of Biomedical Engineering, The Guangdong Key Laboratory for Biomedical Measurements and Ultrasound Imaging, Shenzhen University, Shenzhen, China*
[4]*Department of Psychiatry, University of North Carolina at Chapel Hill, North Carolina*
[5]*Department of Brain and Cognitive Engineering, Korea University, Seoul, Republic of Korea*

◆━━━━━━━━━━━━━━━━━━━━━━━━━━━━━━━━◆
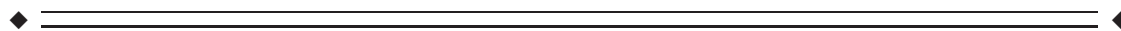
Abstract: The intrinsic relationship between the convoluted cortical folding and the underlying complex whiter matter fiber connections has received increasing attention in current neuroscience studies. Recently, the axonal pushing hypothesis of cortical folding has been proposed to explain the finding that the axonal fibers (derived from diffusion tensor images) connecting to gyri are significantly denser than those connecting to sulci in both adult human and non-human primate brains. However, it is still unclear about the spatiotemporal patterns of the fiber density on the cortical surface of the developing infant brains from birth to 2 years of age, which is the most dynamic phase of postnatal brain development. In this paper, for the first time, we systemically characterized the spatial distributions and longitudinal developmental trajectories of the cortical fiber density in the first 2 postnatal years, via joint analysis of longitudinal structural and diffusion tensor imaging from 33 healthy infants. We found that the cortical fiber density increases dramatically in the first year and then keeps relatively stable in the second year. Moreover, we revealed that the cortical fiber density on gyral regions was significantly higher at 0, 1, and 2 years of age than that on sulcal regions in the frontal, temporal, and parietal lobes. Meanwhile, the cortical fiber density was strongly positively correlated with cortical thickness at several three-hinge junction regions of gyri. These results significantly advanced our understanding of the intrinsic relationship between the cortical folding, cortical thickness and axonal wiring during early postnatal stages. *Hum Brain Mapp 36:5183–5195, 2015.* © 2015 Wiley Periodicals, Inc.

Key words: infant; cortical surface; fiber density; cortical folding; cortical thickness; longitudinal development

◆━━━━━━━━━━━━━━━━━━━━━━━━━━━━━━━━◆

INTRODUCTION

The human cerebral cortex is characterized by the highly convoluted cortical folding, composed of concave sulci and convex gyri [Carman et al., 1995; Ono et al., 1990; Van Essen and Drury, 1997; Zilles et al., 1989], and their underlying complicated axonal connections [Nie et al., 2012a; Van Essen, 1997]. Recently, the intrinsic relationship between these two characteristic attributes has received increasing attention in neuroscience studies, though the answer remains largely unclear. During the third trimester of fetal life, the human cerebral cortex grows dramatically from a relatively smooth, lissencephalic structure into a convoluted structure, largely resembling the morphology of the adult brain [Armstrong et al., 1995; Hill et al., 2010]. It has been hypothesized that the axonal wiring is a critical driving force forming the convoluted cortical folding [Van Essen, 1997]. In recent neuroimaging studies of both adult human and non-human primate brains, the terminations of axonal fibers derived from diffusion tensor imaging (DTI) data were found to dominantly concentrate on convex gyri, relative to the concave sulci [Chen et al., 2013; Li et al., 2010; Nie et al., 2012a]. This finding has also been replicated in a range of mammalian brains via DTI and high angular resolution diffusion imaging (HARDI) [Nie et al., 2012a; Zhang et al., 2014], including the recently released Human Connectome Project data [Zhang et al., 2014]. Moreover, structural fiber connection patterns were found to closely follow gyral folding patterns in the neocortices of macaque, chimpanzee, and human brains, despite the progressively increased complexity and variability of cortical folding and structural connection patterns during evolution [Chen et al., 2013]. In parallel, at the cellular and molecular levels, a recent joint study of the Allen Mouse Brain Connectivity Atlas and the Allen Mouse Brain Atlas demonstrated that the cerebellum gyri and sulci of rodent brains are significantly different in both axonal connectivity and gene expression patterns [Zeng et al., 2014]. However, all these findings cannot be well explained by the popular tension-based theory of morphogenesis, which posits that the cortical regions strongly interconnected by wiring axons are pulled towards one another to form a gyral fold [Van Essen, 1997], thus implying that axonal fibers should concentrate on sulci rather than on gyri. To bridge this significant gap, the axonal pushing hypothesis of cortical folding has been proposed, which implies that gyri should have a higher density of fiber connection than sulci [Chen et al., 2013; Nie et al., 2012a].

However, all prior studies of the cortical fiber density that supported the axonal pushing hypothesis have focused on adult brains, with both cortical folding and axonal wiring being well developed [Chen et al., 2013; Nie et al., 2012a]. Therefore, it is still unclear how the cortical fiber density *spatially* distributes and *longitudinally* develops on the cortical surface of developing infants from birth to 2 years of age, which is the most dynamic and critical phase of postnatal structural and functional development of the human cerebral cortex [Choe et al., 2013; Gao et al., 2009b; Gao et al., 2011; Gilmore et al., 2012; Hazlett et al., 2011; Holland et al., 2014; Knickmeyer et al., 2008; Li et al., 2013; Lyall et al., 2015; Meng et al., 2014; Nie et al., 2012b; Qiu et al., 2015; Sadeghi et al., 2013; Shi et al., 2010]. At term birth, major cortical sulcal-gyral folding and long-range axonal connections are already present [Chi and Dooling, 1976; Dubois et al., 2008a; Hill et al., 2010; Kostovic and Jovanov-Milosevic, 2006; Takahashi et al., 2012]. In the first postnatal year, cortical surface area expands approximately 80% [Li et al., 2013] and cortical thickness increase about 42% [Li et al., 2015a], with regionally heterogeneous growth patterns, accompanied with dynamic white matter myelination and maturation [Geng et al., 2012; Qiu et al., 2015; Sadeghi et al., 2013]. Many neurodevelopmental and neuropsychiatric disorders are hypothesized to be the consequences of abnormal brain development during this critical period of dynamic cortex growth [Gilmore et al., 2012; Grewen et al., 2014; Hazlett et al., 2011; Lyall et al., 2015; Wolff et al., 2012, 2015]. Therefore, studying the cortical fiber density during this period would greatly advance our understanding of the intrinsic relationship between cortical folding and fiber connection during their dynamic development, and also provide important insights into the neurodevelopmental disorders with abnormal cortical folding or axonal connection. Motivated by these reasons, for the first time (as far as we know), this study aims to systematically investigate the spatial distributions and longitudinal development of the cortical fiber density by using 33 healthy infants, each with both longitudinal structural and diffusion tensor imaging scans at birth, 1 year, and 2 years of age. Moreover, the relationship between the cortical fiber density and cortical thickness, which is an important cortical anatomical attribute related to normal development, cognitive functioning, and neurodevelopmental and neuropsychiatric disorders [Fischl and Dale, 2000; Li et al., 2015a; Lyall et al., 2015; Nie et al., 2013; Rimol et al., 2010; Shaw et al., 2006, 2008; Sowell et al., 2004], was also quantitatively characterized across the whole cortex at each of the three ages.

MATERIALS AND METHODS

Subjects

This study was approved by the Institutional Review Board of the University of North Carolina (UNC), Chapel Hill. Pregnant mothers were recruited during the second trimester of pregnancy from the UNC hospitals. Informed written consents were obtained from all parents. Exclusion criteria included abnormalities on fetal ultrasound, gestational age at birth <32 weeks, major medical or neurologic illness after birth, and major medical or psychotic illness in the mother [Gilmore et al., 2012; Yap et al., 2011].

In total, 33 normal developing infants (16 males and 17 females) were included in this study, with each infant being longitudinally scanned three times at 0, 1, and 2 years of age. The gestational ages at MRI scans were: 41.4 ± 1.6 weeks, 94.5 ± 2.4 weeks, and 144.7 ± 4.5 weeks for 0, 1, and 2 years of age, respectively. This infant data-set has been used in previous studies on longitudinal development of cortical structural networks [Nie et al., 2014; Yap et al., 2011].

MR Image Acquisition

Longitudinal T1, T2, and diffusion-weighted MR images were acquired using a Siemens 3T head-only scanner (Allegra, Siemens Medical System, Erlangen, Germany) with a circular polarized head coil. All infants were scanned unsedated while asleep, fitted with ear protection and with their heads secured in a vacuum-fixation device. T1-weighted images (160 sagittal slices) were acquired by using the imaging parameters: TR = 1,900 ms, TE = 4.38 ms, inversion time = 1,100 ms, flip angle = 7°, and resolution = $1 \times 1 \times 1$ mm^3. T2-weighted images (70 transverse slices) were acquired using the parameters: TR = 7,380 ms, TE = 119 ms, flip angle = 150°, and resolution = $1.25 \times 1.25 \times 1.95$ mm^3. Diffusion-weighted images (45 axial slices) were acquired with the parameters: TR/TE = 5,200/73 ms, acquisition matrix = 128×96, voxel resolution = $2 \times 2 \times 2$ mm^3, one image without diffusion gradient ($b = 0$), and six noncollinear diffusion gradient directions at $b = 1,000$ s/mm^2. To improve the signal-to-noise ratio, for each subject, a single DWI volume was obtained by combing five repeated sequences after motion correction.

Image Preprocessing

All images were visually inspected to ensure reasonable quality before analysis. All structural MR images were preprocessed using an infant-specific computational pipeline as detailed in [Li et al., 2013,2014b,2014d]. Briefly, it includes the following major steps: (1) skull stripping by a learning-based method [Shi et al., 2012] and removal of cerebellum and brain stem by registration with an atlas [Shen and Davatzikos, 2002]; (2) correction of intensity inhomogeneity using N3 [Sled et al., 1998]; (3) rigid alignment onto the age-specific infant brain atlas [Shi et al., 2011]; (4) tissue segmentation of infant brain MR images using an infant-dedicated longitudinally-guided coupled level-set method [Wang et al., 2011; Wang et al., 2013a,b]; (5) masking and filling non-cortical structures, and separation of each brain into left and right hemispheres.

For DTI images, after distortion correction, diffusion tensors were first constructed by a weighted least squares estimation method [Basser et al., 1994; Zhu et al., 2007] and the fractional anisotropy (FA) map was then computed [Yap et al., 2011]. Next, a whole-brain streamline

tractography was conducted on each DTI image in its native space with the following parameters: the minimal seed point FA of 0.2, minimal allowed FA of 0.1, maximal turning angle of 70°, minimal fiber length of 20 mm, and maximal fiber length of 200 mm [Yap et al., 2011]. The motivation of using a low FA threshold was to ensure that unmyelinated white matter fibers could be reasonably extracted in infant brains. To align structural images with DTI, for each subject, T2 image was rigidly aligned onto the b0 image. All alignment results were visually inspected to ensure the quality. This transformation matrix was also used to transform cortical surfaces reconstructed from structural images onto the DTI space in the following sections.

Cortical Surface Reconstruction and Registration

Cortical surface reconstruction and registration were performed by an infant-specific computational pipeline for cortical surface-based analysis, which has been extensively verified on more than 500 infant brain MR images [Li et al., 2013,2014a,2014c,2015b; Lyall et al., 2015]. Specifically, for each hemisphere of each image, cortical surfaces represented by triangular meshes were reconstructed by using a topology-preserving deformable surface method [Li et al., 2012, 2014a], based on tissue segmentation results. The inner cortical surface (white-gray matter interface) was first reconstructed by topology correction of the white matter and then tessellation of the corrected white matter as a triangular mesh. To address the severe partial volume effects in the tight sulci of small-sized infant brain MRI, which might result in incorrect reconstruction of the outer cortical surface, explicit thin separations between opposite tight sulci were further recovered [Li et al., 2012, 2014a]. Next, the inner cortical surface was deformed using forces derived from Laplace's equation to reconstruct the outer cortical surface by preserving its initial topology and also avoiding surface mesh self-intersection [Li et al., 2012, 2014a]. The cortical thickness of each vertex was then computed as the average value of the minimum distance from inner to outer surfaces and the minimum distance from outer to inner surfaces. The inner cortical surface was also parcellated as four lobes, i.e., frontal, parietal, temporal, and occipital lobes, and then segmented as sulcal regions and gyral regions [Li et al., 2009], respectively. For cortical surface registration, the inner cortical surface was further smoothed, inflated, and mapped to a sphere by minimizing the metric distortion between the cortical surface and its spherical representation [Fischl et al., 1999].

To determine longitudinal vertex-to-vertex cortical correspondences, for each hemisphere of each subject, its spherical cortical surface at the ith ($i \in 0, 1$) year of age was aligned onto its corresponding cortical surface at the $i + 1$th years of age by using Spherical Demons based on
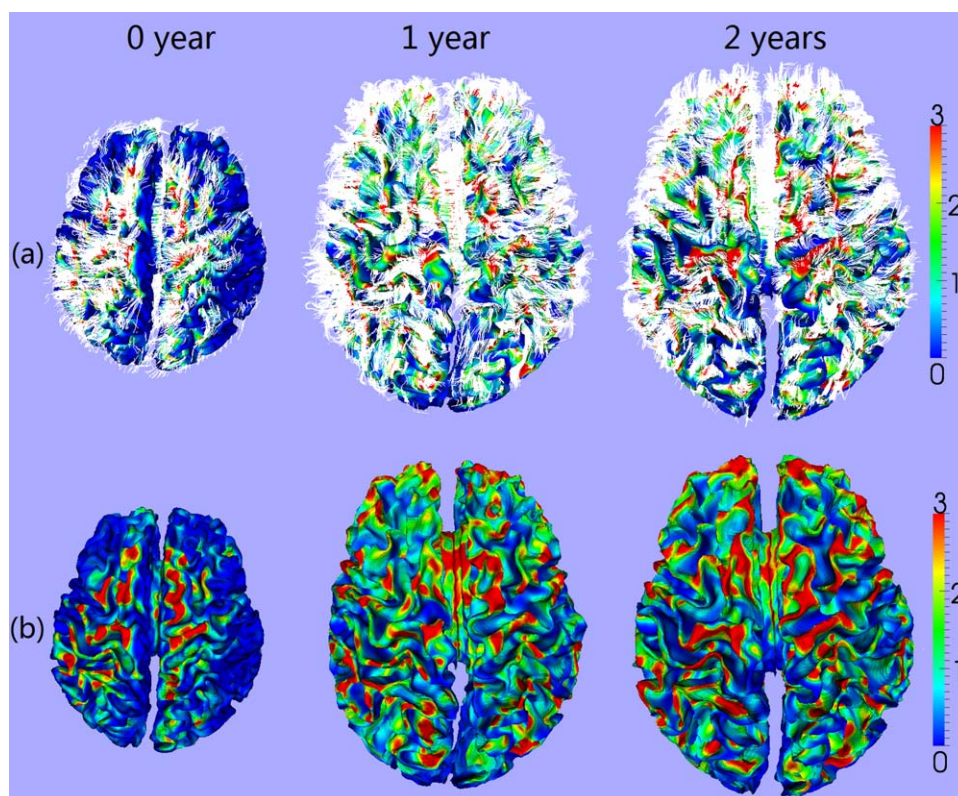
Figure 1.

Cortical fiber density on a representative developing infant at 0, 1, and 2 years of age. (**a**) Overlaying the fibers (white streamlines) with the cortical surfaces. (**b**) Fiber density (mm2) on the cortical surfaces. The color bars are shown on the right. [Color figure can be viewed in the online issue, which is available at wileyonlinelibrary.com.]

the cortical folding geometries [Yeo et al., 2010]. For each hemisphere of each subject, the deformation field from 0 to 2 years of age was then computed by concatenating the deformation map from 0 to 1 year of age and that from 1 to 2 years of age [Li et al., 2013]. To establish unbiased cross-sectional vertex-to-vertex cortical correspondences, for each hemisphere, group-wise registration of spherical cortical surfaces of all subjects at 2 years of age were performed by using Spherical Demons [Yeo et al., 2010]. For each hemisphere, the inner cortical surface of each subject at 2 years of age was resampled to a standard-mesh tessellation based on the deformation field obtained from the group-wise surface registration, thus establishing the vertex-to-vertex correspondences across all subjects at 2 years of age. Based on the longitudinal surface registration results of each subject, the standard-mesh tessellation of each subject at 2 years of age was further warped to 1 year of age and 0 year of age, respectively, thereby establishing the longitudinal vertex-to-vertex cortical correspondences. Hence, for each hemisphere, inner cortical surfaces of all subjects across all ages were represented by the same standard mesh tessellation, thus establishing

both longitudinal and cross-sectional vertex-to-vertex cortical correspondences. All cortical surface reconstruction and registration results have been visually inspected to ensure reasonable quality.

Computing Fiber Density on Cortical Surfaces

Based on the streamline tractography results, fibers were connected onto the resampled inner cortical surfaces to measure the fiber density [Nie et al., 2012a; Zhang et al., 2010]. Note that the extracted fibers could be *either* outside the inner cortical surface when the gray matter is oversegmented, *or* inside the inner cortical surface when the gray matter is undersegmented. To address this issue, if an end point of a fiber is outside of the inner cortical surface, the connection point of this fiber was located by searching along the fiber backwards the inner cortical surface. Otherwise, the connection point was searched by extending the fiber towards the inner cortical surface. The searching procedure stopped either when the connection point was found, or a searching threshold of 20 mm was exceeded
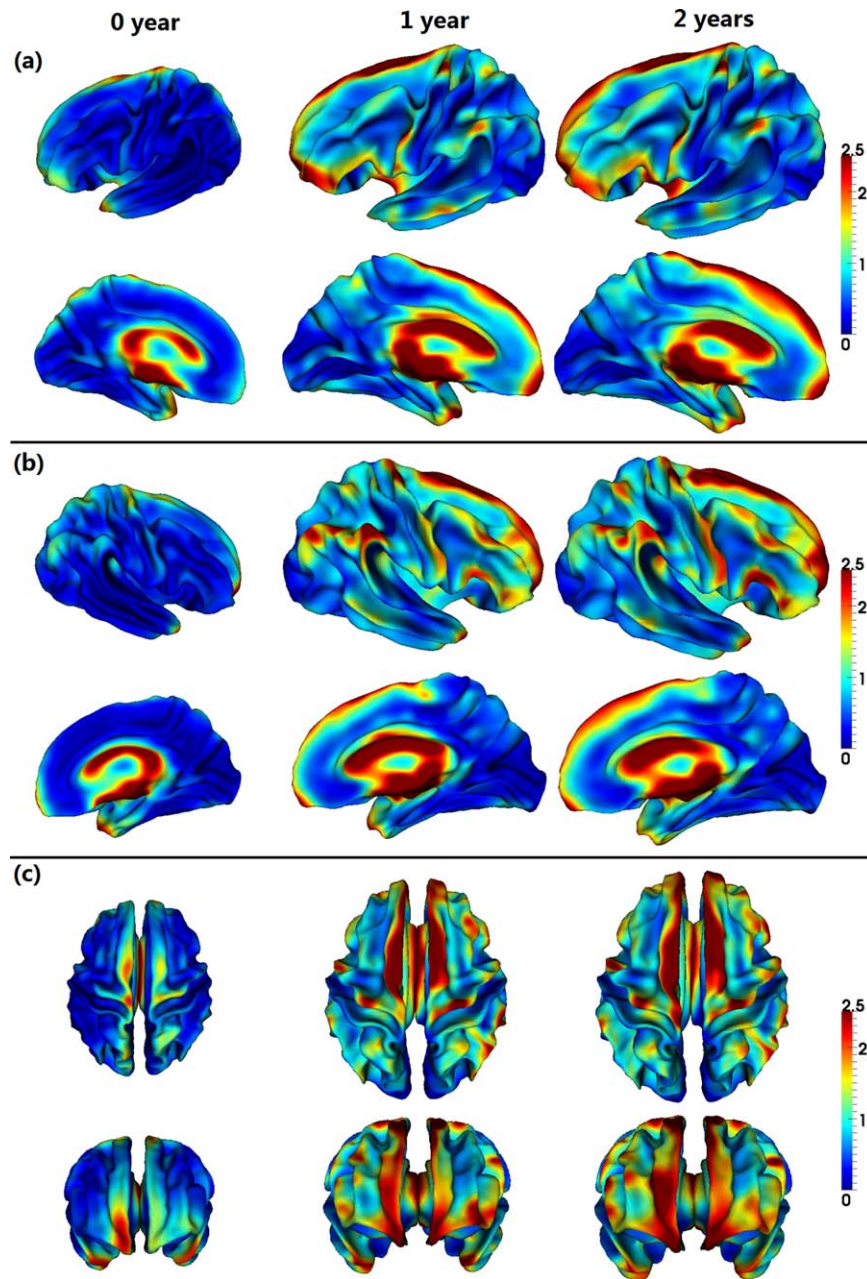
Figure 2.

Spatial distributions of the average fiber density (/mm^2) on cortical surfaces from 33 infants, at 0, 1, and 2 years of age. Warm colors indicate high fiber density, and cold colors indicate low fiber density. [Color figure can be viewed in the online issue, which is available at wileyonlinelibrary.com.]

[Nie et al., 2014]. After the above procedure, any fibers that cannot reach the inner cortical surface were discarded. For each vertex on the inner cortical surface, the fiber density was then defined as the number of fibers connected to a unit area (mm^2). Figure 1 shows the computed cortical fiber density on a representative infant at 0, 1, and 2 years of age.

RESULTS

Spatial Distributions of Cortical Fiber Density at 0, 1, and 2 Years of Age

Figure 2 shows the vertex-wise spatial distribution of the average fiber density on cortical surfaces from 33
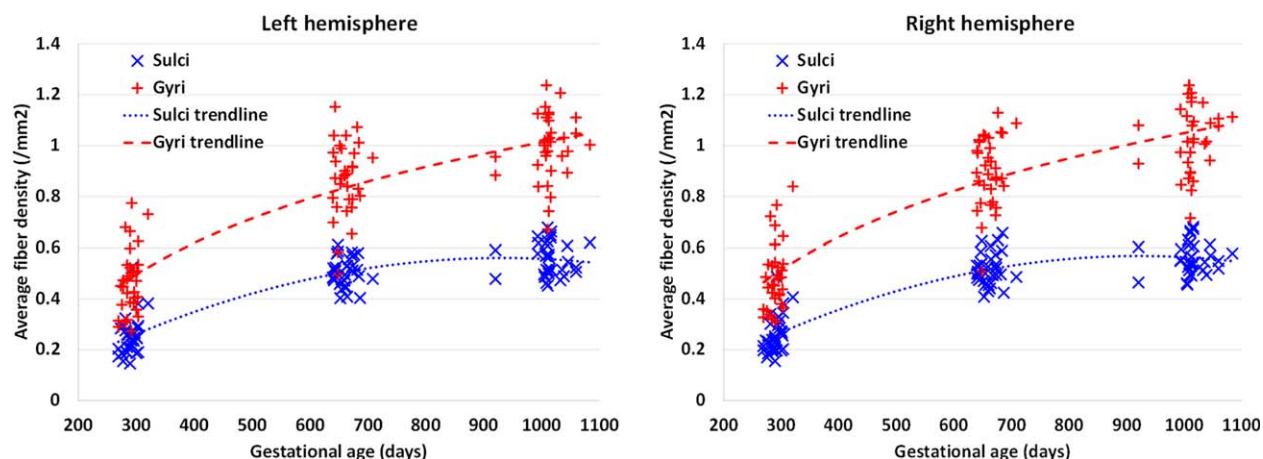
Figure 3.
Scatter plots of the average cortical fiber density in the sulcal and gyral regions, respectively, across the whole cortex of 33 infants at 0, 1, and 2 years of age. [Color figure can be viewed in the online issue, which is available at wileyonlinelibrary.com.]

infants at 0, 1, and 2 years of age. As shown in Figure 2, the cortical surface exhibits regionally heterogeneous patterns of fiber density at the three ages. In general, gyri have higher fiber density than sulci, which is particularly pronounced in the frontal lobe. Figure 3 provides the scatter plots of the average cortical fiber density on sulci and gyri separately across the whole cortex of the 33 subjects. As we can see from Figures 2 and 3, the cortical fiber density increases dramatically in the first year and then increases relatively small in the second year. Specifically, in the first year, the cortical fiber density increases 112% on sulci and 99% on gyri. In contrast, in the second year, the cortical fiber density only increases 10% on sulci and 16% on gyri. To further investigate the region-specific patterns of the cortical fiber density between sulci and gyri, Figure 4 shows the mean and standard deviation of the cortical fiber density on each of the four lobes, i.e., frontal, parietal, temporal, and occipital lobes, and also on the whole cortex from the 33 infants at 0, 1, and 2 years of age. Among the four lobes, the frontal lobe consistently exhibits the highest fiber density on gyri, whereas the occipital lobe consistently shows the lowest fiber density on gyri from 0 to 2 years of age. Table I shows the ratios of the cortical fiber density on gyri versus that on sulci at 0, 1, and 2 years of age. The frontal and temporal cortices consistently exhibit high ratios of the cortical fiber density between gyri and sulci, whereas the occipital cortex consistently exhibits low ratios. Table II further provides the statistical significance of the cortical fiber density difference between gyri and sulci in the first 2 years of age, by using paired t-test. Specifically, in the frontal, temporal, and parietal lobes, the fiber density on gyri is statistically significantly higher than that on sulci ($P < 0.05$) consistently at 0, 1, and 2 years of age. In contrast, in the occipital lobe, there is no significant difference on the fiber density

between sulci and gyri at 0 year of age. Moreover, the fiber density on gyri is even significantly lower than that on sulci on both hemispheres at 1 year of age, and also on the right hemisphere at 2 years of age ($P < 0.05$).

Relationship Between Fiber Density and Cortical Thickness in Infants

Cortical thickness is an important anatomical attribute of the cortex, and is related to normal development and aging, cognitive functioning, and neuropsychiatric disorders [Lyall et al., 2015]. For illustration, Figure 5 provides the scatter plots of the average cortical thickness on sulci and gyri separately across the whole cortex of the 33 subjects. As we can see, cortical thickness increases dramatically in the first year and then changes very subtly in the second year. However, the relationship between the cortical fiber density and cortical thickness has not been studied before. Herein, for the first time, the Pearson's correlation coefficient between these two distinct cortical attributes was computed for each vertex across the whole cortex for each age group, as shown in Figure 6. Note that, before the correlation analysis, a linear regression was performed at each vertex of each age to remove the effects of multiple confounding variables: age, gender and overall mean values [He et al., 2007; Nie et al., 2014]. The residuals were then treated as the raw values for correlation analysis. As we can see from Figure 6, the correlation coefficients of the fiber density and cortical thickness were age-related and regionally heterogeneous across the cortex. Interestingly, many junction regions of gyri, e.g., the junction between percentral and middle temporal gyri, and the junction between percentral and superior temporal gyri, exhibited strong positive correlations between the cortical
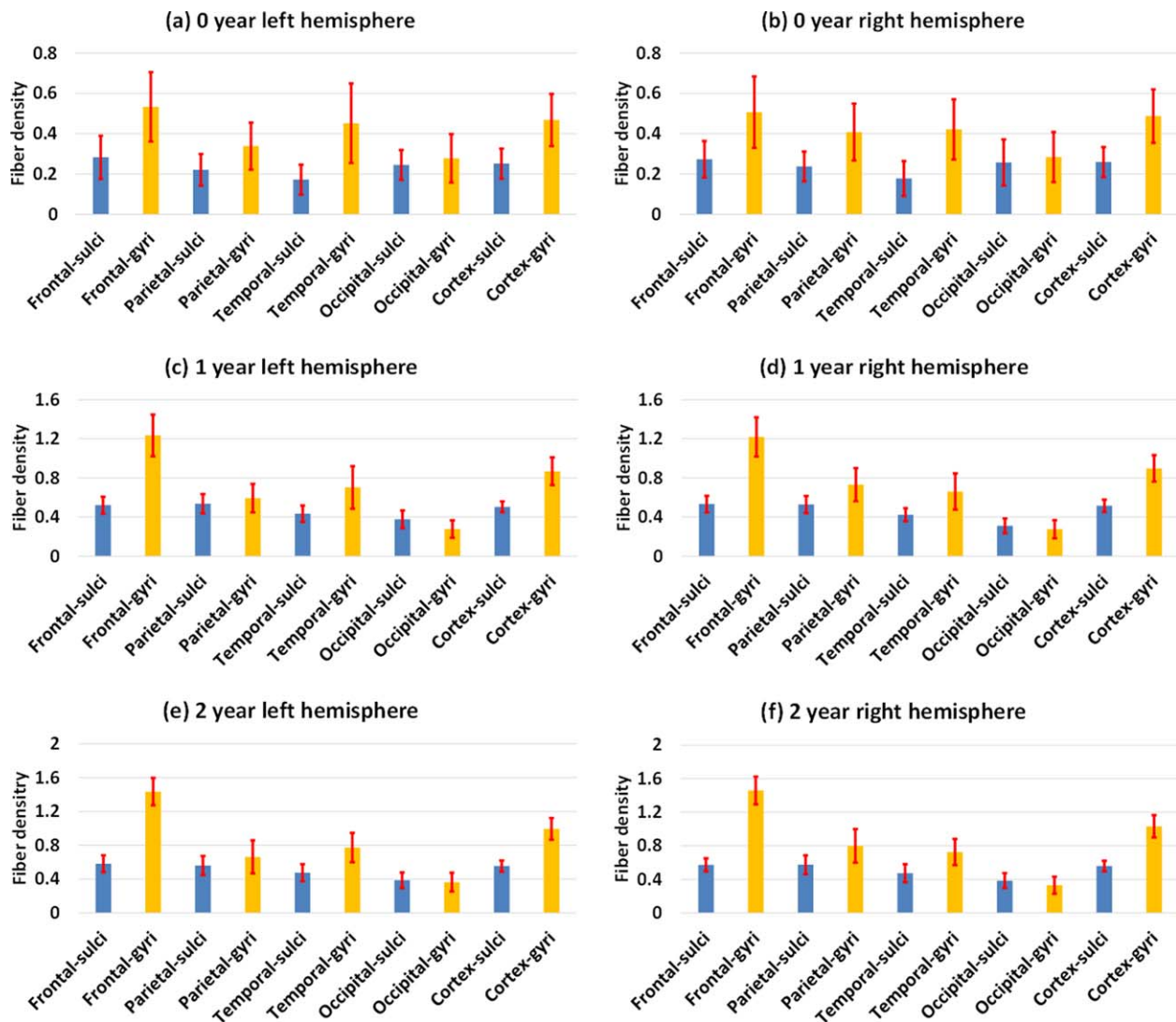
Figure 4.

Means and standard deviations of the cortical fiber density (/mm^2) in the sulcal and gyral regions of four lobes and the whole cortex from 33 infants at 0, 1, and 2 years of age. [Color figure can be viewed in the online issue, which is available at wileyonlinelibrary.com.]

TABLE I. Ratios of the cortical fiber density on gyri versus those on sulci at 0, 1, and 2 years of age

Regions	0 year		1 year		2 years	
	Left	Right	Left	Right	Left	Right
Frontal lobe	2.00 ± 0.69	1.92 ± 0.53	2.46 ± 0.66	2.36 ± 0.58	2.54 ± 0.55	2.61 ± 0.56
Parietal lobe	1.61 ± 0.48	1.78 ± 0.55	1.17 ± 0.41	1.43 ± 0.44	1.28 ± 0.58	1.48 ± 0.56
Temporal lobe	2.87 ± 1.25	2.70 ± 1.17	1.68 ± 0.56	1.61 ± 0.56	1.68 ± 0.48	1.61 ± 0.51
Occipital lobe	1.19 ± 0.54	1.22 ± 0.69	0.74 ± 0.20	0.90 ± 0.25	0.95 ± 0.26	0.87 ± 0.23
Whole cortex	1.91 ± 0.44	1.93 ± 0.40	1.75 ± 0.38	1.77 ± 0.36	1.83 ± 0.39	1.88 ± 0.38

Left: left hemisphere; Right: right hemisphere.

TABLE II. Statistical significance of the cortical fiber density difference between sulci and gyri at 0, 1, and 2 years of age

P Values	0 year		1 year		2 years	
Regions	Left	Right	Left	Right	Left	Right
Frontal lobe	**1.00E-11**	**2.87E-11**	**4.41E-16**	**5.00E-17**	**4.57E-21**	**1.86E-21**
Parietal lobe	**1.04E-07**	**3.79E-09**	**0.0236**	**2.36E-06**	**0.0179**	**4.93E-05**
Temporal lobe	**5.46E-10**	**5.26E-12**	**1.01E-07**	**1.20E-07**	**1.76E-10**	**2.68E-08**
Occipital lobe	0.133	0.206	**9.14E-08**	**0.0295**	0.1972	**0.0029**
Whole cortex	**2.93E-14**	**1.53E-14**	**1.97E-13**	**5.10E-15**	**1.46E-15**	**2.17E-16**

Bold values indicate P values smaller than 0.05.
Left: left hemisphere; right: right hemisphere.

fiber density and cortical thickness in the first 2 years of age, as pointed out by red arrows in Figure 6.

DISCUSSION

It has been shown that the cortical fiber density increased dramatically in the first year and then increased relatively small in the second year. At term birth, although long-range axonal connection are already present [Kostovic and Jovanov-Milosevic, 2006; Takahashi et al., 2012], the white matter has a low degree of myelination [Dubois et al., 2006, 2008b; Geng et al., 2012], thus leading to a small number of fibers approaching the cortex using the streamline fiber tracking. Then, the white matter undergoes dynamic myelination and maturation in the first year, relative to the second year, resulting in much more tracked fibers connecting to the cortex at 1 year and 2 years of age, compared with 0 year of age. The more dynamic increase of the cortical fiber density in the first year relative to the second year is also consistent with the finding that the cortical folding degree

grows more rapidly in the first year than the second year [Li et al., 2014d], indicating the existence of intrinsic relationship between the cortical folding and axonal connectivity. In addition, our result is consistent with the finding that the change of diffusion indices derived from DTI is much more dynamic in the first year than in the second year [Gao et al., 2009a; Geng et al., 2012].

Our results have shown that the cortical fiber density on gyri was significantly higher at 0, 1, and 2 years of age than that on sulci in the frontal, temporal, and parietal lobes, which is consistent with the findings in adult brains and also supports the recent axonal pushing hypothesis of cortical folding [Nie et al., 2012a]. However, in contrast to other lobes, the cortical fiber density on gyri in the occipital lobe (visual cortex) was not significantly different from that on sulci at 0 year of age. Moreover, the fiber density on gyri was significantly lower than that on sulci at 1 year and 2 years of age. This may suggest regionally varying relationship between the cortical folding and axonal wiring, which, however, needs to be further verified in the adult human and nonhuman primate brains. This result
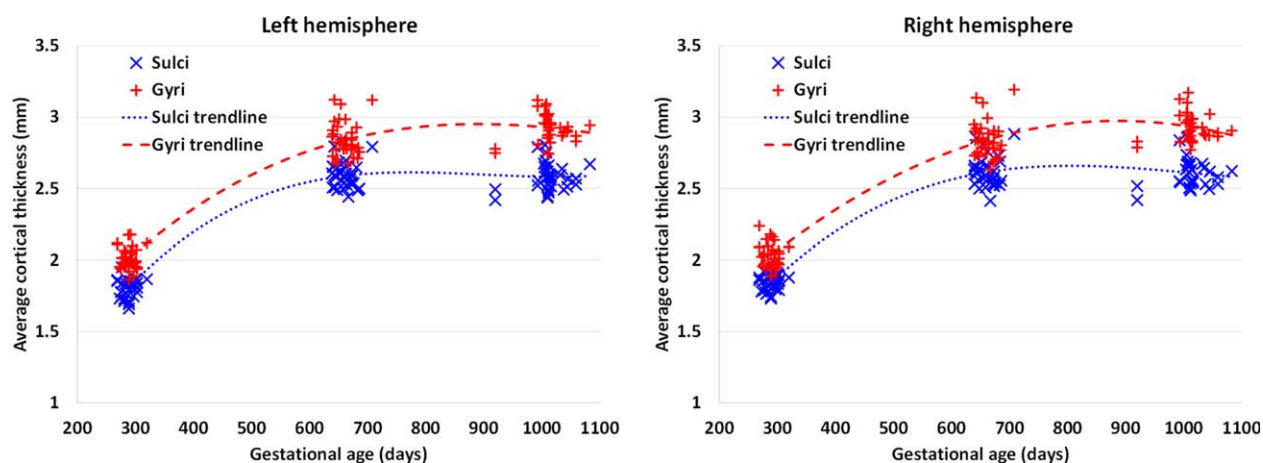

Figure 5.
Scatter plots of the average cortical thickness in the sulcal and gyral regions, respectively, across the whole cortex of 33 infants at 0, 1, and 2 years of age. [Color figure can be viewed in the online issue, which is available at wileyonlinelibrary.com.]
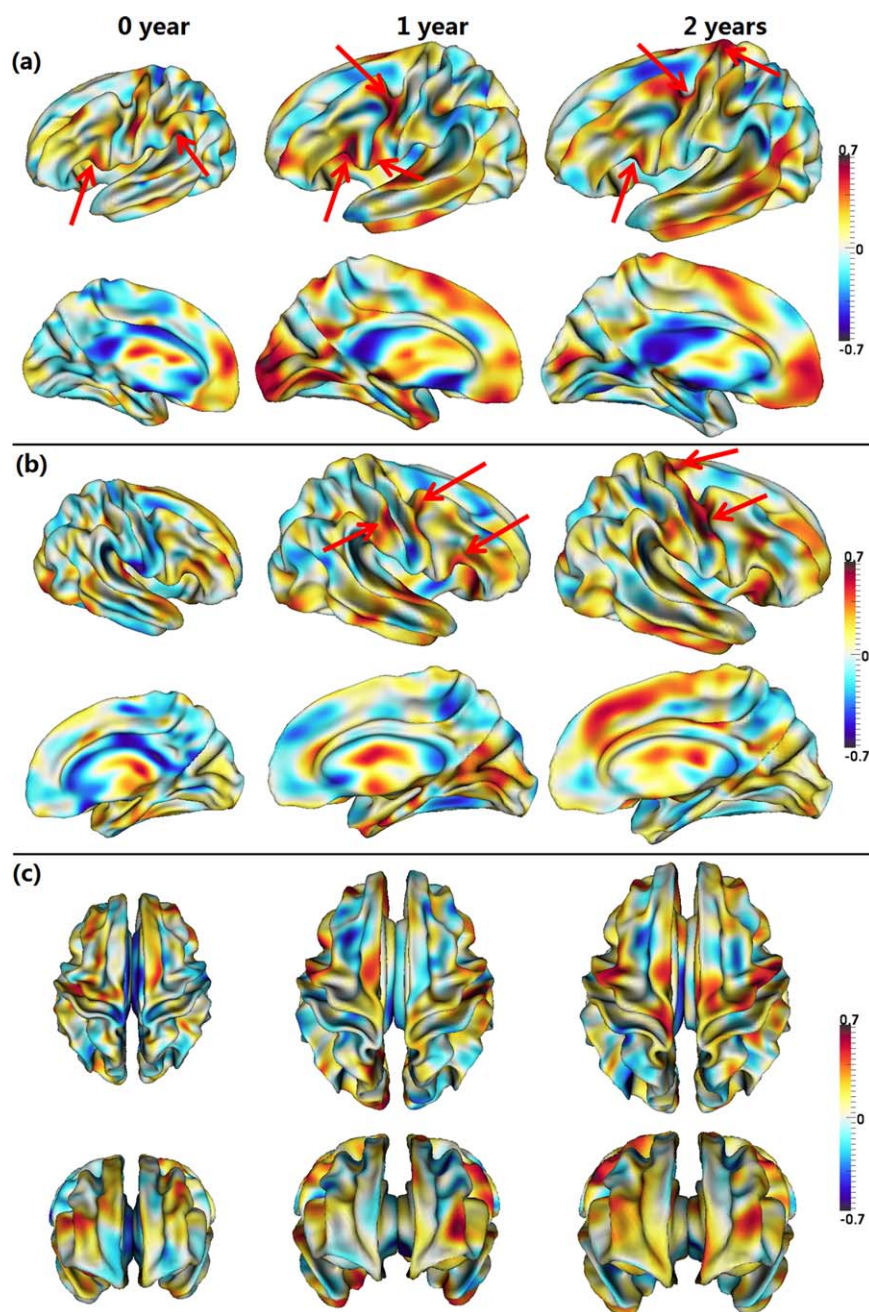
Figure 6.

Pearson's correlation coefficients between the cortical fiber density and cortical thickness from 33 infants at 0, 1, and 2 years of age. Warm colors indicate strong positive correlation, while cool colors indicate strong negative correlation. Red arrows point out several regions with strong positive correlations. Pictures in (a–c) show correlation maps in different views. [Color figure can be viewed in the online issue, which is available at wileyonlinelibrary.com.]

might also suggest that there could be multiple cortical folding mechanisms interacting with each other in different brain areas and during different stages of neurodevelopment [Van Essen, 2013; Zilles et al., 2013]. Notably, the "gyral bias" concept [Van Essen et al., 2014] cannot explain the inverted gyral/sulcal fiber density patterns in the occipital lobe here. And recent studies have suggested that the macro-scale DTI-derived fiber connection patterns

largely agree with the meso-scale axonal connection patterns mapped via anterograde tracers coupled with serial two-photon tomography [Chen et al., 2015].

Similar to the developmental pattern of the cortical fiber density, cortical thickness also increased dynamically in the first year and relatively subtle in the second year [Li et al., 2015a], reflecting the underlying age-specific cytoarchitectural changes of the cortex. Also, cortical thickness on gyri is generally larger than that on sulci in adults [Fischl and Dale, 2000], resembling the spatial distribution of cortical fiber density and also reflecting distinct cortical attributes on sulci and gyri. To assess the underlying relationship between cortical thickness and fiber density, for the first time (as far as we know), we revealed that these two distinct cortical attributes had particularly strong positive correlations in several three-hinge junction regions of gyri, where the fiber density has also been found significantly higher than that in two-hinge gyri in adults [Li et al., 2010]. This result may suggest that the axonal wiring *not only* determines the cortical folding *but also* affects the cortical thickness in these junction regions of gyri, if this can be also replicated in other populations. Again, the "gyral bias" concept [Van Essen et al., 2014] cannot well explain the significantly increased fiber densities on three-hinge junction areas [Li et al., 2010], since typically the surface curvatures in these three-hinge areas are substantially smaller than those two-hinge areas, where more biases should be observed according to the "gyral bias" concept. Instead, we believe that the mapping of DTI-derived fiber densities in those three-hinge gyri reflects the true biological phenomenon. In addition, the negative correlation between tract density and cortical thickness in sulcal regions might suggest a different folding mechanism in sulci other than that in gyri. One possibility is that the stiff fiber tracts in the gyral regions constantly "push" the cortical plate such that the cortical layers have to grow in the tangential directions, thus gradually forming the sulci under the constraint of brain skull. Given the much less dense tract fibers connected in the sulci, more accumulation of neurons in the sulcal regions would result in a negative correlation between tract density and cortical thickness in these areas. We will extensively examine this hypothesis via both neuroimaging data analysis and computational simulation in our future work.

We should mention that, in this article, we studied only the cross-subject correlation, i.e., the correlation between cortical thickness and fiber density across subjects at each vertex of each age group, as we are interested in the spatially-detailed correlation map between these two attributes. In fact, there also exist other two types of correlations: (1) within-subject temporal correlation (i.e., the correlation between cortical thickness and fiber density over all ages for each subject) and (2) within-subject spatial correlation (i.e., the correlation between cortical thickness map and fiber density map for each subject at each age). For example, as shown in Figures 3 and 5, both cortical

thickness and fiber density increase dynamically in the first year, suggesting positive within-subject temporal correlations. However, in the second year, the average cortical thickness in the sulcal regions decreases, while the corresponding fiber density still increases, thus indicating negative within-subject temporal correlations, although these two attributes both increase in the gyral regions. This further suggests differential growth mechanisms between sulci and gyri. In our future work, we will comprehensively study these three types of correlation in the large-scale longitudinal MRI datasets.

It should be caveated that one limitation of our current study is that streamline tractography from DTI has difficulty in accurately dealing with complex crossing fibers [Mori et al., 1999]. Nevertheless, previous studies in adults using advanced stochastic tractography and HARDI found similar distinct patterns of cortical fiber density between gyri and sulci, compared with the case of using streamline tractography, implying that these findings are independent of the tractography methods [Nie et al., 2012a]. Therefore, it is less likely that our findings on cortical fiber density between gyri and sulci in developing infants would change substantially when using stochastic tractography [Behrens et al., 2003], which will be further verified in our future work. However, we should mention that tractography from diffusion MR imaging is an indirect method for studying axonal fibers at the macroscale, which is affected by a set of factors, such as computational simulation methods and their parameter settings, and also the limited imaging resolutions. Hence, it is possible that some complicated axonal fibers, such as crossing fibers and U-shape fibers, cannot be revealed by the existing tractography studies. Also, the highly folded nature of the cortical surface might further cause false positives/negatives when fiber tracking approaches the cortex [Reveley et al., 2015]. Essentially, current diffusion imaging techniques are far from being able to accurately map the *complete* complex fiber pathways and connectional architectures of the cerebral cortex [Markov et al., 2011; Schmahmann and Pandya, 2006; Thomas et al., 2014], although some studies in animals have demonstrated substantial similarities between diffusion imaging derived fiber pathways and invasive tracer injection results [Azadbakht et al., 2015; Dauguet et al., 2007; Dyrby et al., 2007; Jbabdi et al., 2013], which are frequently considered as the golden standard for the fiber pathways. With the availability of large-scale neuronal tracing data, such as the Allen Mouse Brain Connectivity Atlas (http://connectivity.brain-map.org), it becomes feasible to evaluate and validate DTI and DTI tractography methods based on the benchmark data of high-density axonal projections mapped by microscopic serial two-photon tomography [Chen et al., 2015]. In addition, DTI tractography methods and parameters could be potentially optimized in order to maximize both sensitivity and specificity of mapping real axons via the golden standard of neuronal tracing data, as shown in our recent study [Chen et al., 2015].

In summary, for the first time (as far as we are aware), we systemically characterized the spatial distributions and longitudinal developmental trajectories of cortical fiber density in the first 2 postnatal years, via joint analysis of longitudinal structural and diffusion tensor MRI data from 33 healthy infants. We revealed several hitherto unseen patterns of cortical fiber density during the dynamic early postnatal stages, including (1) cortical fiber density increased dramatically in the first postnatal year and then changed relatively small in the second postnatal year; (2) cortical fiber density on gyri was significantly higher at 0, 1, and 2 years of age than that on sulci in the frontal, temporal, and parietal lobes; and (3) cortical fiber density was strongly positively correlated with cortical thickness at several junction regions of gyri. As all prior studies of cortical folding and axonal wiring in human brains have been largely focused on well-developed adults, our results on the developing infants significantly advance our understanding on the intrinsic relationship between cortical folding and axonal wiring in early postnatal stages, and also provide new evidence that largely supports the axonal pushing hypothesis of cortical folding [Chen et al., 2013; Nie et al., 2012a].

REFERENCES

Armstrong E, Schleicher A, Omran H, Curtis M, Zilles K (1995): The ontogeny of human gyrification. Cereb Cortex 5:56–63.

Azadbakht H, Parkes LM, Haroon HA, Augath M, Logothetis NK, de Crespigny A, D'Arceuil HE, Parker GJ (2015): Validation of high-resolution tractography against in vivo tracing in the macaque visual cortex. Cereb Cortex, In Press.

Basser PJ, Mattiello J, Lebihan D (1994): Estimation of the effective self-diffusion tensor from the NMR spin-echo. J Magn Reson Ser B 103:247–254.

Behrens TEJ, Johansen-Berg H, Woolrich MW, Smith SM, Wheeler-Kingshott CAM, Boulby PA, Barker GJ, Sillery EL, Sheehan K, Ciccarelli O, Thompson AJ, Brady JM, Matthews PM (2003): Non-invasive mapping of connections between human thalamus and cortex using diffusion imaging. Nat Neurosci 6:750–757.

Carman GJ, Drury HA, Van Essen DC (1995): Computational methods for reconstructing and unfolding the cerebral cortex. Cereb Cortex 5:506–517.

Chen H, Liu T, Zhao Y, Zhang T, Li Y, Li M, Zhang H, Kuang H, Guo L, Tsien JZ (2015): Optimization of large-scale mouse brain connectome via joint evaluation of DTI and neuron tracing data. Neuroimage 115:202–213.

Chen H, Zhang T, Guo L, Li K, Yu X, Li L, Hu X, Han J, Liu T (2013): Coevolution of gyral folding and structural connection patterns in primate brains. Cereb Cortex 23:1208–1217.

Chi JG, Dooling EC (1976): Gyral development of the human brain. Trans Am Neurol Assoc 101:89–90.

Choe MS, Ortiz-Mantilla S, Makris N, Gregas M, Bacic J, Haehn D, Kennedy D, Pienaar R, Caviness VSJ, Benasich AA, et al. (2013): Regional infant brain development: An MRI-based morphometric analysis in 3 to 13 month olds. Cereb Cortex 23: 2100–2117.

Dauguet J, Peled S, Berezovskii V, Delzescaux T, Warfield SK, Born R, Westin CF (2007): Comparison of fiber tracts derived from in-vivo DTI tractography with 3D histological neural tract tracer reconstruction on a macaque brain. Neuroimage 37:530–538.

Dubois J, Benders M, Cachia A, Lazeyras F, Ha-Vinh Leuchter R, Sizonenko SV, Borradori-Tolsa C, Mangin JF, Huppi PS (2008a): Mapping the early cortical folding process in the preterm newborn brain. Cereb Cortex 18:1444–1454.

Dubois J, Dehaene-Lambertz G, Perrin M, Mangin JF, Cointepas Y, Duchesnay E, Bihan Hertz-Pannier LDL (2008b): Asynchrony of the early maturation of white matter bundles in healthy infants: Quantitative landmarks revealed noninvasively by diffusion tensor imaging. Hum Brain Mapp 29:14–27.

Dubois J, Hertz-Pannier L, Dehaene-Lambertz G, Cointepas Y, Le Bihan D (2006): Assessment of the early organization and maturation of infants' cerebral white matter fiber bundles: A feasibility study using quantitative diffusion tensor imaging and tractography. Neuroimage 30:1121–1132.

Dyrby TB, Sogaard LV, Parker GJ, Alexander DC, Lind NM, Baare WF, Hay-Schmidt A, Eriksen N, Pakkenberg B, Paulson OB, et al. (2007): Validation of in vitro probabilistic tractography. Neuroimage 37:1267–1277.

Fischl B, Dale AM (2000): Measuring the thickness of the human cerebral cortex from magnetic resonance images. Proc Natl Acad Sci USA 97:11050–11055.

Fischl B, Sereno MI, Dale AM (1999): Cortical surface-based analysis. II: Inflation, flattening, and a surface-based coordinate system. Neuroimage 9:195–207.

Gao W, Lin W, Chen Y, Gerig G, Smith JK, Jewells V, Gilmore JH (2009a): Temporal and spatial development of axonal maturation and myelination of white matter in the developing brain. AJNR Am J Neuroradiol 30:290–296.

Gao W, Zhu H, Giovanello KS, Smith JK, Shen D, Gilmore JH, Lin W (2009b): Evidence on the emergence of the brain's default network from 2-week-old to 2-year-old healthy pediatric subjects. Proc Natl Acad Sci USA 106:6790–6795.

Gao W, Gilmore JH, Giovanello KS, Smith JK, Shen D, Zhu H, Lin W (2011): Temporal and spatial evolution of brain network topology during the first two years of life. PLoS One 6:e25278.

Geng X, Gouttard S, Sharma A, Gu H, Styner M, Lin W, Gerig G, Gilmore JH (2012): Quantitative tract-based white matter development from birth to age 2 years. Neuroimage 61:542–557.

Gilmore JH, Shi F, Woolson SL, Knickmeyer RC, Short SJ, Lin W, Zhu H, Hamer RM, Styner M, Shen D (2012): Longitudinal development of cortical and subcortical gray matter from birth to 2 years. Cereb Cortex 22:2478–2485.

Grewen K, Burchinal M, Vachet C, Gouttard S, Gilmore JH, Lin W, Johns J, Elam M, Gerig G (2014): Prenatal cocaine effects on brain structure in early infancy. Neuroimage 101:114–123.

Hazlett HC, Poe MD, Gerig G, Styner M, Chappell C, Smith RG, Vachet C, Piven J (2011): Early brain overgrowth in autism associated with an increase in cortical surface area before age 2 years. Arch Gen Psychiatry 68:467–476.

He Y, Chen ZJ, Evans AC (2007): Small-world anatomical networks in the human brain revealed by cortical thickness from MRI. Cereb Cortex 17:2407–2419.

Hill J, Dierker D, Neil J, Inder T, Knutsen A, Harwell J, Coalson T, Van Essen D (2010): A surface-based analysis of hemispheric asymmetries and folding of cerebral cortex in term-born human infants. J Neurosci 30:2268–2276.

Holland D, Chang L, Ernst TM, Curran M, Buchthal SD, Alicata D, Skranes J, Johansen H, Hernandez A, Yamakawa R, et al. (2014): Structural growth trajectories and rates of change in the first 3 months of infant brain development. JAMA Neurol 71: 1266–1274.

Jbabdi S, Lehman JF, Haber SN, Behrens TE (2013): Human and monkey ventral prefrontal fibers use the same organizational principles to reach their targets: Tracing versus tractography. J Neurosci 33:3190–3201.

Knickmeyer RC, Gouttard S, Kang C, Evans D, Wilber K, Smith JK, Hamer RM, Lin W, Gerig G, Gilmore JH (2008): A structural MRI study of human brain development from birth to 2 years. J Neurosci 28:12176–12182.

Kostovic I, Jovanov-Milosevic N (2006): The development of cerebral connections during the first 20-45 weeks' gestation. Semin Fetal Neonatal Med 11:415–422.

Li G, Guo L, Nie J, Liu T (2009): Automatic cortical sulcal parcellation based on surface principal direction flow field tracking. Neuroimage 46:923–937.

Li G, Nie J, Wu G, Wang Y, Shen D (2012): Consistent reconstruction of cortical surfaces from longitudinal brain MR images. Neuroimage 59:3805–3820.

Li G, Nie J, Wang L, Shi F, Lin W, Gilmore JH, Shen D (2013): Mapping region-specific longitudinal cortical surface expansion from birth to 2 years of age. Cereb Cortex 23:2724–2733.

Li G, Nie J, Wang L, Shi F, Gilmore JH, Lin W, Shen D (2014a): Measuring the dynamic longitudinal cortex development in infants by reconstruction of temporally consistent cortical surfaces. Neuroimage 90:266–279.

Li G, Nie J, Wang L, Shi F, Lyall AE, Lin W, Gilmore JH, Shen D (2014b): Mapping longitudinal hemispheric structural asymmetries of the human cerebral cortex from birth to 2 years of age. Cereb Cortex 24:1289–1300.

Li G, Wang L, Shi F, Lyall AE, Ahn M, Peng Z, Zhu H, Lin W, Gilmore JH, Shen D (2014c): Cortical thickness and surface area in neonates at high risk for schizophrenia. Brain Struct Funct. In Press.

Li G, Wang L, Shi F, Lyall AE, Lin W, Gilmore JH, Shen D (2014d): Mapping longitudinal development of local cortical gyrification in infants from birth to 2 years of age. J Neurosci 34:4228–4238.

Li G, Lin W, Gilmore JH, Shen D (2015a): Spatial patterns, longitudinal development, and hemispheric asymmetries of cortical thickness in infants from birth to 2 years of age. J Neurosci 35: 9150–9162.

Li G, Wang L, Shi F, Gilmore JH, Lin W, Shen D (2015b): Construction of 4D high-definition cortical surface atlases of infants: Methods and applications. Med Image Anal 25:22–36.

Li K, Guo L, Li G, Nie J, Faraco C, Cui G, Zhao Q, Miller LS, Liu T (2010): Gyral folding pattern analysis via surface profiling. Neuroimage 52:1202–1214.

Lyall AE, Shi F, Geng X, Woolson S, Li G, Wang L, Hamer RM, Shen D, Gilmore JH (2015): Dynamic development of regional cortical thickness and surface area in early childhood. Cereb Cortex 25:2204–2212.

Markov NT, Misery P, Falchier A, Lamy C, Vezoli J, Quilodran R, Gariel MA, Giroud P, Ercsey-Ravasz M, Pilaz LJ, et al. (2011): Weight consistency specifies regularies of macaque cortical networks. Cereb Cortex 21:1254–1272.

Meng Y, Li G, Lin W, Gilmore JH, Shen D (2014): Spatial distribution and longitudinal development of deep cortical sulcal landmarks in infants. Neuroimage 100:206–218.

Mori S, Crain BJ, Chacko VP, van Zijl PC (1999): Three-dimensional tracking of axonal projections in the brain by magnetic resonance imaging. Ann Neurol 45:265–269.

Nie J, Guo L, Li K, Wang Y, Chen G, Li L, Chen H, Deng F, Jiang X, Zhang T, et al. (2012a): Axonal fiber terminations concentrate on gyri. Cereb Cortex 22:2831–2839.

Nie J, Li G, Shen D (2013): Development of cortical anatomical properties from early childhood to early adulthood. Neuroimage 76:216–224.

Nie J, Li G, Wang L, Gilmore JH, Lin W, Shen D (2012b): A computational growth model for measuring dynamic cortical development in the first year of life. Cereb Cortex 22:2272–2284.

Nie J, Li G, Wang L, Shi F, Lin W, Gilmore JH, Shen D (2014): Longitudinal development of cortical thickness, folding, and fiber density networks in the first 2 years of life. Hum Brain Mapp 35:3726–3737.

Ono M, Kubik S, Abernathey CD (1990): Atlas of the Cerebral Sulci, Vol. xiv. New York: Thieme Medical Publishers. pp 218.

Qiu A, Mori S, Miller MI (2015): Diffusion tensor imaging for understanding brain development in early life. Annu Rev Psychol 66:853–876.

Reveley C, Seth AK, Pierpaoli C, Silva AC, Yu D, Saunders RC, Leopold DA, Ye FQ (2015): Superficial white matter fiber systems impede detection of long-range cortical connections in diffusion MR tractography. Proc Natl Acad Sci USA 112: E2820–E2828.

Rimol LM, Hartberg CB, Nesvag R, Fennema-Notestine C, Hagler DJ Jr, Pung CJ, Jennings RG, Haukvik UK, Lange E, Nakstad PH, et al. (2010): Cortical thickness and subcortical volumes in schizophrenia and bipolar disorder. Biol Psychiatry 68:41–50.

Sadeghi N, Prastawa M, Fletcher PT, Wolff J, Gilmore JH, Gerig G (2013): Regional characterization of longitudinal DT-MRI to study white matter maturation of the early developing brain. Neuroimage 68:236–247.

Schmahmann JD, Pandya DN. 2006. Fiber Pathways of the Brain, Vol. xviii. Oxford, NY: Oxford University Press. pp 654.

Shaw P, Kabani NJ, Lerch JP, Eckstrand K, Lenroot R, Gogtay N, Greenstein D, Clasen L, Evans A, Rapoport JL, et al. (2008): Neurodevelopmental trajectories of the human cerebral cortex. J Neurosci 28:3586–3594.

Shaw P, Lerch J, Greenstein D, Sharp W, Clasen L, Evans A, Giedd J, Castellanos FX, Rapoport J (2006): Longitudinal mapping of cortical thickness and clinical outcome in children and adolescents with attention-deficit/hyperactivity disorder. Arch Gen Psychiatry 63:540–549.

Shen D, Davatzikos C (2002): HAMMER: Hierarchical attribute matching mechanism for elastic registration. IEEE Trans Med Imaging 21:1421–1439.

Shi F, Yap PT, Fan Y, Gilmore JH, Lin W, Shen D (2010): Construction of multi-region-multi-reference atlases for neonatal brain MRI segmentation. Neuroimage 51:684–693.

Shi F, Wang L, Dai Y, Gilmore JH, Lin W, Shen D (2012): LABEL: Pediatric brain extraction using learning-based meta-algorithm. Neuroimage 62:1975–1986.

Shi F, Yap PT, Wu G, Jia H, Gilmore JH, Lin W, Shen D (2011): Infant brain atlases from neonates to 1- and 2-year-olds. PLoS One 6:e18746.

Sled JG, Zijdenbos AP, Evans AC (1998): A nonparametric method for automatic correction of intensity nonuniformity in MRI data. IEEE Trans Med Imaging 17:87–97.

Sowell ER, Thompson PM, Leonard CM, Welcome SE, Kan E, Toga AW (2004): Longitudinal mapping of cortical thickness and brain growth in normal children. J Neurosci 24:8223–8231.

Takahashi E, Folkerth RD, Galaburda AM, Grant PE (2012): Emerging cerebral connectivity in the human fetal brain: an MR tractography study. Cereb Cortex 22:455–464.

Thomas C, Ye FQ, Irfanoglu MO, Modi P, Saleem KS, Leopold DA, Pierpaoli C (2014): Anatomical accuracy of brain connections derived from diffusion MRI tractography is inherently limited. Proc Natl Acad Sci USA 111:16574–16579.

Van Essen DC (1997): A tension-based theory of morphogenesis and compact wiring in the central nervous system. Nature 385: 313–318.

Van Essen DC (2013): Cartography and connectomes. Neuron 80: 775–790.

Van Essen DC, Drury HA (1997): Structural and functional analyses of human cerebral cortex using a surface-based atlas. J Neurosci 17:7079–7102.

Van Essen DC, Jbabdi S, Sotiropoulos SN, Chen C, Dikranian K, Coalson T, Harwell J, Behrens TEJ, Glasser MF. 2014. Mapping connections in humans and nonhuman primates: Aspirations and challenges for diffusion imaging. In: Johansen-Berg H, Behrens TEJ, editors. Diffusion MRI: From Quantitative Measurement to In-Vivo Neuroanatomy, 2nd ed. London, UK: Elsevier/Academic Press.

Wang L, Shi F, Lin W, Gilmore JH, Shen D (2011): Automatic segmentation of neonatal images using convex optimization and coupled level sets. Neuroimage 58:805–817.

Wang L, Shi F, Li G, Gao Y, Lin W, Gilmore JH, Shen D (2013a): Segmentation of neonatal brain MR images using patch-driven level sets. Neuroimage 84C:141–158.

Wang L, Shi F, Yap PT, Lin W, Gilmore JH, Shen D (2013b): Longitudinally guided level sets for consistent tissue segmentation of neonates. Hum Brain Mapp 34:956–972.

Wolff JJ, Gerig G, Lewis JD, Soda T, Styner MA, Vachet C, Botteron KN, Elison JT, Dager SR, Estes AM, et al. (2015): Altered corpus callosum morphology associated with autism over the first 2 years of life. Brain 138:2046–2058.

Wolff JJ, Gu H, Gerig G, Elison JT, Styner M, Gouttard S, Botteron KN, Dager SR, Dawson G, Estes AM, et al. (2012): Differences in white matter fiber tract development present from 6 to 24 months in infants with autism. Am J Psychiatry 169:589–600.

Yap PT, Fan Y, Chen Y, Gilmore JH, Lin W, Shen D (2011): Development trends of white matter connectivity in the first years of life. PLoS One 6:e24678.

Yeo BT, Sabuncu MR, Vercauteren T, Ayache N, Fischl B, Golland P (2010): Spherical demons: Fast diffeomorphic landmark-free surface registration. IEEE Trans Med Imaging 29:650–668.

Zeng T, Chen H, Fakhry A, Hu X, Liu T, Ji S (2014): Allen mouse brain atlases reveal different neural connection and gene expression patterns in cerebellum gyri and sulci. Brain Struct Funct 220:2691–2703.

Zhang DG, Guo L, Li G, Nie JX, Deng F, Li KM, Hu XT, Zhang T, Jiang X, Zhu DJ, et al. (2010): Automatic cortical surface parcellation based on fiber density information. In: 7th IEEE International Symposium on Biomedical Imaging: From Nano to Macro, IEEE, Rotterdam, Netherlands. pp 1133–1136.

Zhang T, Chen H, Guo L, Li K, Li L, Zhang S, Shen D, Hu X, Liu T (2014): Characterization of U-shape streamline fibers: Methods and applications. Med Image Anal 18:795–807.

Zhu HT, Zhang HP, Ibrahim JG, Peterson BS (2007): Statistical analysis of diffusion tensors in diffusion-weighted magnetic resonance imaging data. J Am Stat Assoc 102:1085–1102.

Zilles K, Armstrong E, Moser KH, Schleicher A, Stephan H (1989): Gyrification in the cerebral cortex of primates. Brain Behav Evol 34:143–150.

Zilles K, Palomero-Gallagher N, Amunts K (2013): Development of cortical folding during evolution and ontogeny. Trends Neurosci 36:275–284.